# Developing the Structure of a Cu CMP Model

J. Seok[*], C. P. Sukam[*], L. Borucki[**], A. Jindal[+], J. A. Tichy[*], R. J. Gutmann[+], and T. S. Cale[+]
[*]Dept of Mechanical, Aerospace and Nuclear Engineering
[**]Intelligent Planar, 3831 E. Ivy St., Mesa, AZ 85205
[+]Focus Center - New York, Rensselaer: Interconnections for Gigascale Integration
Rensselaer Polytechnic Institute, Troy NY 12180 USA
seokj@alum.rpi.edu

***Abstract*:** This paper discusses how we are using Cu CMP data to develop a Cu CMP model. CMP data were taken on a non-rotating wafer using a representative dual axis rotational polisher. The data are first analyzed using a mechanical model that incorporates Preston's law, rough surface contact mechanics, thin film fluid mechanics and basic load and moment balances. The limited success of this mechanical model, which was targeted at oxide CMP, motivated us to identify model elements that improve our understanding, including non-Prestonian behavior of the slurry and a thermally activated material removal process; i.e., chemically dominated. These model features were combined with simple mechanical model feature (load and moment balances), to successfully explain experimental observations.

***Keywords:*** CMP, removal rate (RR), contact stress analysis, thermal analysis.

## I. INTRODUCTION

Though widely used in industry, and with a large body of empirical results, the physics of CMP is still not well understood. Some of our recent efforts have provided theoretical tools for understanding the mechanical interactions between the pad and wafer. Tichy *et al*. [1] introduced an elastohydrodyamic model of slurry flow between the rough pad and the wafer to explain experimental observations of suction pressure. Kim *et al*. [2] presented a hyperelastic model for asperity deformation [3], and Seok *et al*. [4] included abrasive particles trapped between asperities and the wafer to explain material removal rate (RR) [5] for CMP processes which are dominated by mechanical phenomena.

In this work, we evaluate whether the above CMP model can be used to model Cu CMP. We use experimental results obtained from CMP experiments on a stationary (non-rotating) wafer on a dual axis CMP tool. A non-rotating wafer was used to avoid the rotationally induced averaging of RR, which results in a more thorough test for a model. We first use a three-dimensional mechanical model that includes asperity and bulk pad deformation, a lubrication model for slurry flow, carrier film deformation, wafer compliance, and material removal by abrasive particles in the slurry. The RR results could not be explained by this model. We then solve an "inverse problem" to infer non-observable CMP variables such as fluid film thickness, fluid pressures and contact pressures from the experimentally obtained RR, using the same model structure. The modeling results reinforce the inadequacy of the mechanical model for Cu CMP. As this model was targeted towards mechanically dominated CMP processes, this is not surprising. Two primary phenomena that were deemed important to predict Cu CMP uniformity in our non-rotating wafer experiments, and that are not included in the mechanical model are: 1) the non-Prestonian behavior of the slurry, and 2) the nonuniformity in the wafer temperature. Including these phenomena in a model that also includes mechanical features such as load and moment balances, can explains the prominent features of the experimental data.

## II. EXPERIMENTAL

Each wafer used was a 125 mm prime silicon wafer on which a 1.7 μm thick blanket copper film was deposited using physical vapor deposition (PVD) onto a 50 nm layer of PVD tantalum ($Cu/Ta/SiO_2/Si$). CMP was performed using an IPEC 372M rotary polisher, a commercial copper damascene first step alumina-based slurry with a mean particle diameter of 25 nm, and Rodel IC-1400 pads; one with XY grooves and the other without grooves. The process conditions are within process windows used to polish Cu in practice (*ex-situ* conditioning, 5 PSI, 90 RPM), except that the back-pressure, arm oscillation and carrier rotation velocity were set to zero.

For each pad type, a single wafer was polished continuously for 5 minutes and a second wafer was polished for 5 one minute intervals. Initially, and after each polishing step, the thickness of the film was measured using a Tencor OmniMap RS50/e resistivity mapper. Total and intermediate mean removal rates were calculated based on the thickness before and after polishing, at 225 regularly distributed test points on the wafer. Film surface quality was evaluated optically and with profilometry after post-CMP cleaning. The initial location of the wafer flat relative to the head and pad was the same for each wafer and was verified at the end of CMP.

Figs. 1(a), (b) and (c) show the measured film thickness at t=0, t=1 and t=4 minutes for the plain pad. Figs. 2 (a), (b) and (c) contain the corresponding data for the XY pad. These figures depict the wafer as seen from above with the pad center to the left and the pad rotating clockwise (in the negative y direction, or "6 o'clock"). Initially the Cu film is thinner toward the pad center and thicker toward the outside edge. After one minute, however, this pattern reverses and a step down in thickness forms that persists for the remainder of the polishing. At the outside edge of the wafer, particularly for the plain pad, there is a reduction in the material removal rate that is evident between the 2 and 4 o'clock positions. The wafer surface also contains deep circular scratches to the right of the y-axis (Fig. 1(a)) that definitively confirm the direction of the pad center.

## III. THE MECHANICAL MODEL

### A. *Model Description*

Details of the mechanical model used have been described elsewhere [2]; only a summary of the pertinent features is given here. The model assumes that the local rate of change of the film thickness *F(x,y)* is given by a local version of Preston's law [6],

$$\dot{F} = k_p V_s \sigma_{G-W} \ , \tag{1}$$

where $V_s$ is the local relative sliding speed between the wafer and the pad, $\sigma_{G-W}$ is the local contact stress, and $k_p$ is a constant. The constant $k_p$ incorporates factors such as the slurry particle diameter and the hardness of the wafer [7]. The local sliding speed $V_s$ at radius $r$ from the pad center for a non-rotating wafer is $V_s = \Omega\, r$, where $\Omega$ is the pad rotation rate. The local contact stress is computed using a Greenwood and Williamson-style model [8],

$$\sigma_{G-W} = \frac{\gamma_1 E_a}{1-\nu_a^2} \eta r_a^{\gamma_2} \int_h^\infty (z-h)^{\gamma_3} \psi(z) dz \ , \tag{2}$$

where $E_a$ and $\nu_a$ are the asperity Young's modulus and Poisson ratio, respectively, $\eta$ is the number of asperities per unit area, $r_a$ is the mean asperity tip radius, $\gamma_i$ $(i = 1, 2, 3)$ are constants for a hyperelastic stress-strain model for asperity deformation [2], $\psi(z)$ is the asperity height probability density function, and $h$ is the local separation between the wafer and the mean plane of the pad surface, which is approximately the same as the fluid thickness. The fluid thickness and fluid pressure $p_f$ are related by the 2D Reynolds equation [9],

$$\nabla \cdot \left( h^3 \varphi_p \nabla p_f \right) = 6\mu \nabla \cdot \left( (h + s\varphi_s) \vec{V}_s \right), \tag{3}$$

where $\mu$ is the viscosity, $\varphi_p$ and $\varphi_s$ are the pressure and shear flow factor corrections (respectively) that are used to include the effects of rough surfaces [10], and $s$ is the RMS roughness of the pad surface. Locally, the sum of the contact stress from (2) and the fluid pressure from (3) is balanced by the stress $\sigma_w(x,y)$ at the surface of the bulk pad material. The integral of the latter over the wafer surface must equal the applied load. Furthermore, in the CMP tool used, the external load is applied through a pivot point that cannot transmit a moment. Hence, the moment due to local friction forces must be balanced by the moment produced by the normal stresses at the bulk pad surface.

### B. *Inverse Problem Iterative Scheme*

Results of direct or forward simulations using this model were qualitatively different than experimental observations. To check whether the model itself (and not just inaccurate parameter values) is to blame for the performance of the model, we pursued inverse analysis. In this case, we seek to determine if we can start with measured data, and part of the model, and then generate reasonable predictions of intermediate variable values. We use the following iterative method to analyze RR data. First we guess the Preston coefficient in (1). Given the measured average removal rate and the known sliding speed, we obtain the local contact stress using (1). The local fluid thicknesses are then calculated from (2), and the corresponding fluid pressure field is calculated from (3). Application of load balance then provides a correction for the Preston coefficient. The converged values of the fluid pressures, asperity contact stresses and fluid film thickness are used to evaluate the bulk pad deformations and the actual shape of the deformed wafer. Good convergence is obtained after a few iterations.

### C. *Mechanical Model Results*

For the plain pad, Figures 3 (a) and (b) present, respectively, the calculated interfacial slurry film thicknesses and pressure profiles. The solid contact pressure $\sigma_{G-W}$ (not shown) is higher toward the outside of the pad and follows the material removal rate, as one would expect from Eqn. (1) and the known sliding speed. The corresponding fluid film thickness from Eqn. (2) (See Fig. 3(a)) varies most in the direction normal to the sliding velocity. The converged solution of the two-dimensional Reynolds equation shows that the resulting fluid pressure field (Fig. 3(b)) is subambient, except near the outermost edge. Hence, high compression at the thinnest film region causes high suction pressures. The positive pressures that occur near the outermost edge of the wafer would play the role of lifting the edge and reducing the contact stresses.

The predicted fluid pressures and film thicknesses are not reasonable when compared with the RR data. Thus, we conclude that the mechanical model does not have the right structure, or model features. That does not mean that it is entirely incorrect; out interpretation is that the model is incomplete. For example, there are no terms that deal with chemisty in the model, and it would be surprising if if worked for Cu CMP. Especially when comparing against data from a non-rotating wafer.

## IV. THERMAL PLUS MECHANICAL MODEL

Following the recognition that the mechanical model does not hold the full explanation, additional model features were explored. For example, a plot of average RR vs. applied pressure for the slurry used show that the rate increases exponentially up to 5 PSI and then levels off. These data were obtained using a rotating wafer experiment (Fig. 4(a)) and a different pad, but indicates that the assumption of local Prestonian behavior may not be reasonable. The RR data may be viewed in another way. At constant rotation rate, the pressure is proportional to the increase in wafer temperature at any fixed time. Thus, the RR curve for the slurry could be reinterpreted as an RR vs. temperature plot. The saturation of the RR with pressure could then be viewed as a possible effect of reactant depletion. Since it is known that the rate of copper removal is sensitive to temperature [11], the expermental results may then be largely a thermal effect. The orientation of the high removal rate region relative to the pad center and the curved shape of the step from the low to high removal rate regions also suggest a thermal effect.

The scenario that this suggests is that, initially, higher contact forces due to film thickness nonuniformity combined with higher sliding speeds at the outside edge of the wafer lead to more rapid removal there. The time scale to reach steady state, assuming a constant coefficient of friction on a polyurethane pad, is on the order of 10-20 seconds [12]. Thus, this is consistent with the development of the low area towards the outside of the wafers in Figs. 1(b) and 2(b) in the first minute. Formation of the outer low area has two side effects; 1) it lowers the solid contact pressure, and 2) it may increase the fluid thickness (a prediction of the mechanical model that seems valid). Additional cooling of the wafer that results from having a thicker film may account for the observed increase in film thickness near the outer perimeter in Fig 1(b),(c), but more work needs to done to improve our understanding of this aspect of the data.

A quantitive test of this theory was performed using an existing thermal model that includes frictional heating of the pad and wafer, 3D heat transfer in the wafer/carrier film/head assembly, cooling of the wafer by the slurry, convection of heat outward on the pad by the slurry, and heat exchange between the slurry and a plain or grooved pad [13]. A load balance and a moment balance at a pivot point near the head face were combined with the thermal model to provide locally varying contact pressure and frictional forces. This provides position dependend heat generation, which depends upon local forces. A material removal rate model based on the RR vs. pressure calibration curve in Fig. 4(a) was also implemented. Computed temperatures and contact pressures are shown in Fig. 4(b), (c). The wafer temperature is primarily radially-dependent, and the model produces a step in film height similar to the observed step. The location of the step is furthermore related to the saturation pressure for the slurry. Thus, the model is consistent with the thermal scenario. A thermal origin for the result suggests a number of predictions that are currently in the process of being tested.

## V. CONCLUSION

We applied a mechanical model, developed for oxide polishing, as an inverse procedure to try to explain non-rotating wafer copper removal rate data. While this was not successful, the failure was instructive in that it helped motivate and narrow down the search for the missing physics. This led to an alternative model that includes wafer heating, which affects chemical reaction rates, as well as an observed nonlinear slurry response. These model features, when combined with load and moment balances, successfully explained experimental Cu CMP data. Such efforts, that include both forward and inverse modeling, help design experiments to elucidate model features that are important to specific applications. For example, the two models discussed, as well as features from other models might be combined to cover CMP processes that are dominated by mechanical as well as those dominated by chemical phenomena.

## ACKNOWLEDGMENT

The authors gratefully acknowledge support for this work from NYSTAR, DARPA and MARCO through the Interconnect Focus Center, Silicon Quest International for the wafers and Rodel for the pads. Useful discussions with Mike Oliver (Rodel) are gratefully acknowledged.

## REFERENCES

[1] J. Tichy, J. Levert, L. Shan and S. Danyluk, “Contact mechanics and lubrication hydrodynamics of chemical mechanical polishing,” *J. Electrochem. Soc.*, vol. 146 (4), pp. 1523-1528, 1999.

[2] A. T. Kim, J. Seok, C. P. Sukam, J. T. Tichy and T. S. Cale, “A multiscale model for chemical mechanical planarization,” in *Advanced Metallization Conference 2001*, A. McKerrow, Y. Shacham-Diamand, S. Zaima, T. Ohba, Eds., MRS, 2001, pp. 405-410.

[3] K.L. Johnson, *Contact Mechanics*, Cambridge University Press, Cambridge, UK, 1985.

[4] J. Seok, C. P. Sukam, A. T. Kim, J. A. Tichy and T. S. Cale, “Multiscale material removal modeling of chemical mechanical polishing”, *Wear Journal*, vol. 254 (3-4), pp. 307-320, 2003.

[5] J. Seok, C. P. Sukam, A. T. Kim, J. A. Tichy and T. S. Cale, “An integrated multiscale mechanical model for chemical mechanical planarization,” in *Advanced Metallization Conf. 2002*, B. M. Melnick, T. S. Cale, S. Zaima and T. Ohta, Eds., MRS, 2002, pp. 109-114.

[6] F.W. Preston, “The Theory and Design of Plate Glass Polishing Machines”, *J. Soc. Glass Technol.*, vol. 11, pp. 214-256, 1927.

[7] H. Liang, F. Kaufman, R. Sevilla and S. Anjur, “Wear phenomena in chemical mechanical polishing,” *Wear Journal*, vol. 211, pp. 271-279, 1997.

[8] J.A. Greenwood and J.B.P. Williamson, “Contact of nominally flat surfaces,” *Proc. Roy. Soc. London*, vol A295, pp. 300-319, 1966.

[9] B.J. Hamrock, *Fundamentals of Fluid Film Lubrication*, McGraw-Hill, 1994.

[10] N. Patir and H. S. Cheng, “Application of Average Flow Model to Lubrication between Rough Sliding Surfaces,” *J. Lubrication Technol.*, vol. 101, pp. 220-230, 1979.

[11] P. Renteln, T. Ninh, “An Exploration of the Copper CMP Removal Mechanism,” MRS Symp. Proc. Vol. 566, p. 155.

[12] L. Borucki, Z. Li, A. Philipossian, “Heating and Convection in Copper Polishing,” submitted to the 204th meeting of the ECS.

[13] L.Borucki, L.Charns, A. Philipossian, “Analysis of Frictional Heating in Plain and Grooved CMP Polishing Pads,” submitted to the 204th meeting of the ECS.

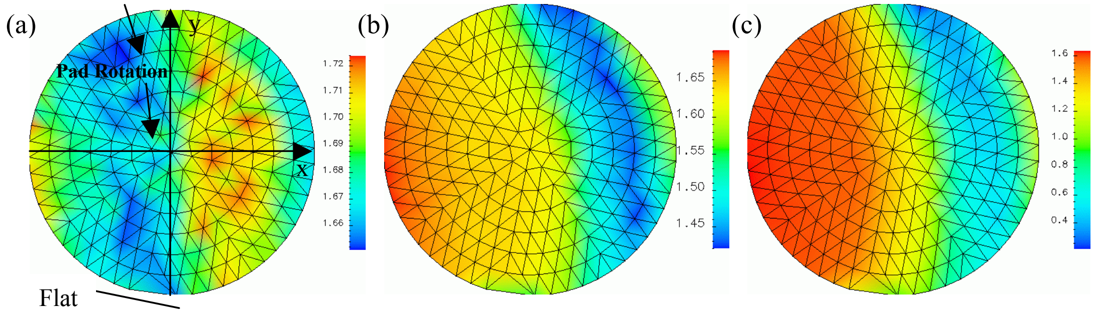

Figure 1. Measured Cu film thickness, plain pad, initially (a), and after 1 and 4 minutes (b), (c). The scales show the film thickness in microns. The pad center is at the left of the wafer center and the flat is indicated.

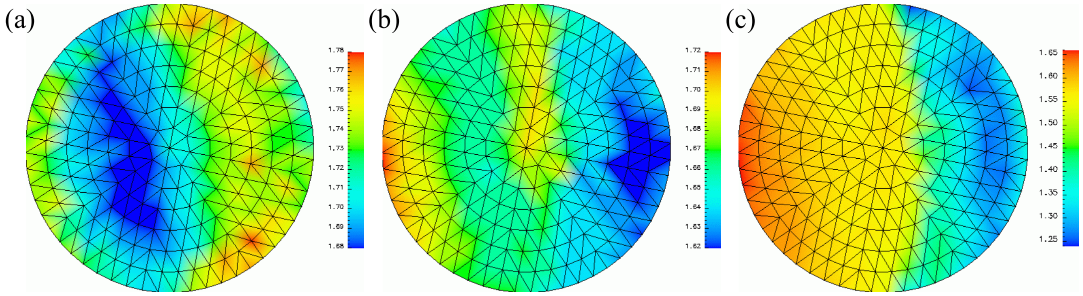

Figure 2. Measured Cu film thickness, XY-groove pad, initially (a), and after 1 and 4 minutes (b), (c).

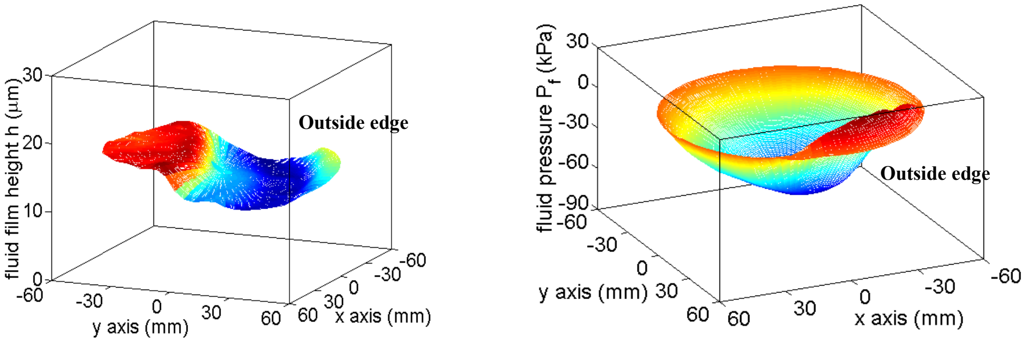

Figure 3. Calculated slurry fluid film thickness *h*, and pressure $p_f$ (plain pad) using the mechanical model.

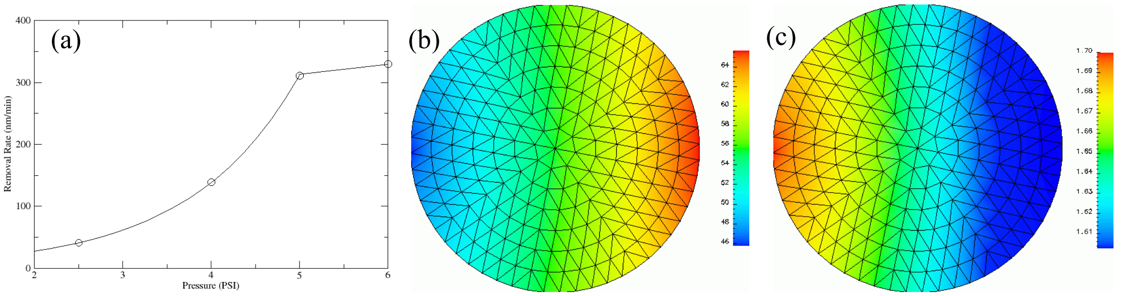

Figure 4. (a) Cu removal rate vs. pressure calibration curve. (b) Calculated wafer temperature. (c) Calculated film thickness from the thermal model with nonlinear removal based on (a).